E/*Z* Conformation and the Vibrational Spectroscopy of $Me_2NN(O)=NOMe$

D. Scott Bohle,*,‡ Joseph Ivanic,† Joseph E. Saavedra,§ Kamilah N. Smith,‡ and Yan-Ni Wang†

Advanced Biomedical Computing Center, SAIC Frederick, National Cancer Institute at Frederick, Frederick, Maryland 21702, Department of Chemistry, McGill University, Montreal, Quebec H3A 2K6, Canada, and Chemistry Section, Basic Research Program, SAIC Frederick, National Cancer Institute at Frederick, Frederick, Maryland 21702

Received: August 22, 2005; In Final Form: October 7, 2005

The simple neutral diazenium diolate, O^2-methyl-1-(*N*, *N*-dimethylamino)diazen-1-ium-1,2-diolate, [$Me_2NN(O)=NOMe$], was experimentally examined by vibrational spectroscopy and the results compared to the theoretically calculated values in an effort to detect both *Z* and *E* conformers which result from the stereochemistry of the N=N multiple bond. Room-temperature Raman and infrared spectra were measured and the results compared with the values calculated theoretically with MP2 and density functional techniques (B3LYP). An analysis of the observed frequencies suggests that, down to a detection limit of about $^1/_{1000}$, only a small quantity of trans (*E*) diazeniumdiolate, <0.05%, may be present at room temperature.

Introduction

In recent years, it has been established that nitric oxide (NO) is a ubiquitous bioregulatory agent, involved in a variety of physiological functions.[1−4] Nitric oxide participates in processes ranging from vasodilation, platelet aggregation, neurotransmission, and immune modulation.[5] As a result of these findings, there has been an increased interest in nitric oxide chemistry and biochemistry. Many nitrogen-bound diazeniumdiolate ions **1** have been shown to hydrolyze under physiological conditions to release 2 equiv of NO, and thus represent a versatile class of nitric oxide donors. On the other hand, the *E* isomer **2** remains unknown as a nonring condensed product. The fundamental properties of these biologically relevant compounds have been extensively investigated and reviewed.[1]

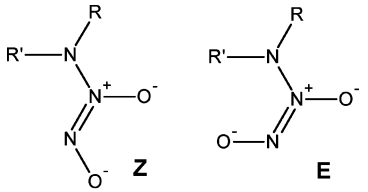

(**1**) (**2**)

To date, all nitrogen-bound diazeniumdiolates have a planar O−N−N−O system and all but one[6] contain oxygen in a *Z* (cis) configuration, **1**, with respect to the N−N double bond. Despite the fact that the formation of carbon-based diazeniumdiolates has been known for many years,[7,8] only a handful of examples[6,9−14] of the *E* (trans) configuration analogues of **2** have been observed. These examples involve cyclic ring systems with N/O disubstitution. Theoretical studies have demonstrated that the acyclic ions are nearly equienergetic with minima corresponding to cis, **1**, and trans, **2**, geometries,[15,16] and therefore could adopt the trans configuration, **2**. Theoretical (B3LYP/aug-cc-pVDZ) rotation barriers for the *O*-alkyl derivatives MeHNN(O)=NOMe and $Me_2NN(O)=NOMe$ are very high, 40.8 and 39.6 kcal/mol, respectively. Furthermore, polarized continuum model (PCM) calculations for the effect of solvation in water suggest that barriers remain high, 36.5 and 37.8 kcal/mol, respectively. Therefore, the absence of **2** in this class of compounds is unlikely to be due to facile isomerization from a product under a thermodynamically controlled reaction. Rather, the most likely rationalization of the preference for the *Z* geometry in **1** is that the product distribution is kinetically controlled.

Herein, we explore a diazeniumdiolate with the structure $R^1R^1NN(O)=NOR^1$, where $R^1 = CH_3$; prior theoretical investigations on similar diazeniumdiolates have indicated that these species could adopt the *E* or *Z* configuration.[6,16−18] Our previous attempts to isolate and observe the *E* isomer of acyclic N-bound diazeniumdiolates by ^{1}H NMR did not provide any conclusive evidence of its existence,[6,16] down to the detection ratio of $^1/_{100}$. In principle, vibrational spectroscopy is a useful tool to analyze the conformation of these ions, and we hypothesized that Raman spectroscopy might allow for *E*-isomer detection due to the anticipated brightness of the symmetric framework modes. In addition, there are considerable advances in the application of Raman spectroscopy to analytical chemistry.[19]

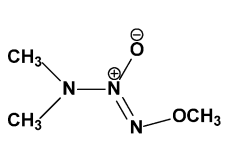

(**3**)

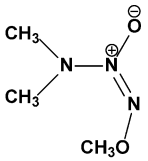

(**4**)

In this paper, Raman and infrared (FT-IR) spectra for the simplest monoalkylated diazeniumdiolate, *Z*-O^2-methyl-1-(*N*,*N*-dimethylamino)diazen-1-ium-1,2-diolate **3**, are presented. The experimental vibrational modes are compared to density functional theory calculations at the B3LYP/aug-cc-pVDZ level for both the *Z* and *E* isomers. The results are then used to identify and quantify the remarkably small fraction of **4**, the previously unreported, and still putative, *E* form of an acyclic nitrogen-bound diazeniumdiolate.

* E-mail: scott.bohle@mcgill.ca.
† Advanced Biomedical Computing Center, SAIC Frederick.
‡ McGill University.
§ Chemistry Section, Basic Research Program, SAIC Frederick.

10.1021/jp054730a CCC: $30.25
Published on Web 11/15/2005

Experimental Section

General. Compound **3**, [$Me_2NN(O)$═NOMe], was prepared from sodium 1-(*N*,*N*-dimethylamino)diazen-1-ium-1,2-diolate and characterized as previously described.[16,20] Briefly, sodium 1-(*N*,*N*-dimethylamino)diazen-1-ium-1,2-diolate, 1.95 g (0.015 mol), was dissolved in 20 mL of methanol, cooled to 0 °C, treated with 1.5 mL (0.016 mol) of dimethyl sulfate, and kept overnight at 25 °C. The product was concentrated on a rotary evaporator, extracted with dichloromethane, washed with water, dried over sodium sulfate, filtered, and evaporated. A vacuum distillation at 50−51 °C at approximately 1 mm Hg gave O^2-methyl-1-(*N*,*N*-dimethylamino)diazen-1-ium-1,2-diolate as a colorless liquid: ^{1}H NMR δ 3.0 (s, 6 H), 4.01 (s, 3H); ^{13}C NMR δ 42.89, 60.85; $UV_{(water)}$ λ_{max} (ϵ) 234 nm (6.8 mM^{-1} cm^{-1}).

Computational Details. Computations were carried out at the restricted Hartree−Fock (RHF), density functional theory (DFT), and second-order Møller−Plesset (MP2) levels of theory.[21,22] DFT calculations used the hybrid B3LYP functional.[23] We have used the aug-cc-pVDZ basis set in all cases, as this basis contains diffuse functions which allow for more reliable electronic descriptions of anions and electron-rich species.[24] Only spherical components of the Cartesian *d* functions were used. Vibrational frequencies were calculated for the optimized structures **3** and **4** along with their Raman intensities.

Vibrational Spectroscopy. Raman spectra were recorded as neat samples on glass slides using a laser intensity of 400 mW. Multiple scan and signal-averaged spectra were collected on a Kaiser Raman spectrometer. Infrared spectra were collected in potassium bromide windows, on a Perkin-Elmer model MB100 Fourier-transform infrared (FT-IR) spectrometer at 1 cm^{-1} resolution. In all cases, data processing was done using the Grams/32 package from Galactic Industries Corporation.

Results

Vibrational Spectroscopy. Given the fact that only five trans diazeniumdiolates have been observed, we have decided to examine O^2-methyl-1-(*N*,*N*-dimethylamino)diazen-1-ium-1,2-diolate [$Me_2NN(O)$═NOMe], a simple nitrogen-bound diazeniumdiolate, in the hopes of obtaining spectroscopic evidence of the presence of the elusive trans isomer or to ascertain an upper limit of its apparently low concentration. Previous reports have noted that only the cis isomer is observed for acyclic nitrogen-bound diazeniumdiolates.[16] To date, only a general vibrational analysis for diazeniumdiolate anions such as **1** and **2** has been reported.[17] The experimentally observed values (FT-Raman and IR), along with the relative intensities of the bands, are compared to the calculated frequencies and are presented in Tables 1−6. In all of these tables, the calculated values for the DFT results are shown. There was very good agreement between DFT and MP2, as can be seen from the values for the MP2 calculations collected in the data tables in the Supporting Information. Both methods agree on the nature of the vibrations, and so, the calculated relative intensities are likely to reflect the relative amounts of the *Z* and *E* isomers.

Band and Isomer Assignments. Because of the absence of an inversion center of symmetry in **3** and **4**, all bands in both the Raman and infrared spectra are allowed. As can be seen in Figures 1−3, there is excellent correspondence between the observed frequencies in both spectra. Note that the KBr optics in the spectrometer limited the IR assignments to bands greater than 600 cm^{-1}. As a consequence, the low-energy data presented in Table 1 are limited to the Raman observations. In addition to the excellent match of observed bands in the IR and the Raman, the experimental frequencies also agree quite closely with the predicted DFT and MP2 vibrational frequencies. All band assignments in Tables 1−6 are based on the relative band energy and the calculated relative Raman and infrared intensities. Previously, it was demonstrated that diazeniumdiolates have strong coupling of the vibrational modes for the substituents

TABLE 1: Observed and Calculated Low-Energy Raman Bands[a]

assigned vib. mode	calculated (cis)		calculated (trans)		Raman exptl		$Raman_{(cis)}$ Δcalcd−exptl	$Raman_{(trans)}$ Δcalcd−exptl
ν_{1t}			347.2	w				
ν_{1c}	353.7	w			353.6	m	0.1	
ν_{2c}	380.0	w			382.7	s	2.7	
ν_{3c}, ν_{2t}	387.3	w	387.7	w				
ν_{3t}			420.9	w	414.3	w		6.6
ν_{4c}	439.1	w			434.3	m	4.8	
*					524.5	w		
ν_{5c}, ν_{4t}	552.9	w	555.8	w	546.2	w	6.7	9.6
ν_{6c}	591.2	w			586.1	m	5.1	

[a] All bands given in cm^{-1} with relative intensities given as w (weak), m (medium), or s (strong). The assigned numbers are listed in order of increasing energy for t (trans) isomer and c (cis). *Not observed.

TABLE 2: Observed and Calculated Fingerprint Region Raman Bands[a]

assigned vib. mode	calculated (cis)		calculated (trans)		Raman exptl		$Raman_{(cis)}$ Δcalcd−exptl	$Raman_{(trans)}$ Δcalcd−exptl
*			665.9	w	675.5	w		9.6
ν_{7c}, ν_{5t}	688.3	w	691.2	w	690.7	w	2.4	0.5
ν_{6t}			764.1	w				
ν_{8c}	883.4	w			866.1	m	17.3	
ν_{7t}			946.3	w				
ν_{9c}	973.3	w			952.1	w	21.2	
ν_{8t}			1001.9	w				
ν_{10c}	1030.6	m			1005.7	s	24.9	
*					1028.8	w		
ν_{11c}, ν_{9t}	1045.8	w	1040.7	w	1035.1	w	10.7	5.6
*					1054.3	m		
ν_{10t}			1064.2	w				
ν_{12c}, ν_{11t}	1097.4	w	1100.7	w	1107.0	w	9.6	6.3
ν_{13c}	1106.7	w			1115.1	w	8.4	
ν_{14c}, ν_{12t}	1149.7	w	1150.4	w	1141.7	m	8.0	8.7
ν_{15c}, ν_{13t}	1156.1	w	1158.3	w	1158.2		2.1	0.1
ν_{14t}			1195.8	w	1197.8			2.0
ν_{16c}	1213.1	w						
ν_{15t}			1231.6	w	1223.5	m		8.1
ν_{17c}, ν_{16t}	1255.9	w	1255.9	w	1259.6	m	3.7	3.7
ν_{18c}	1270.2	w						
ν_{19c}	1295.3	s						
ν_{17t}			1352.2	m	1349.6	m		2.6
*					1364.0	m		
*					1373.9	m		
ν_{20c}, ν_{18t}	1410.3	w	1413.6	w	1402.8	m	7.5	10.8
ν_{21c}, ν_{19t}	1435.9	w	1437.6	w	1435.0	m	0.9	2.6
ν_{22c}, ν_{20t}	1445.6	w	1447.9	w				
ν_{23c}, ν_{21t}	1451.9	w	1450.0	w	1449.8	m	2.1	0.2
ν_{24c}, ν_{22t}	1456.0	w	1454.2	w				
ν_{25c}, ν_{23t}	1470.6	w	1469.4	w				
ν_{26c}	1472.9	w						
ν_{27c}, ν_{24t}	1474.9	w	1475.3	w				
ν_{25t}			1478.6	w				
ν_{26t}			1488.5	w				
ν_{28c}	1493.0	w			1493.6	w	0.6	
*					1497.9	w		
ν_{27t}			1546.0	m				
ν_{29c}	1573.1	m						

[a] All bands given in cm^{-1} with relative intensities given as w (weak), m (medium), or s (strong). The assigned numbers are listed in order of increasing energy for t (trans) isomer and c (cis). *Not observed.

TABLE 3: Observed and Calculated C−H Stretching Region Raman Bands[a]

assigned vib. mode	calculated (cis)		calculated (trans)		Raman exptl		Raman$_{(cis)}$ Δcalcd−exptl	Raman$_{(trans)}$ Δcalcd−exptl
ν_{30c}	2900.1	s			2793.2	w		
ν_{31c}, ν_{28t}	3005.9	s	3000.0	s	2829.3	w		
ν_{32c}, ν_{29t}	3026.0	s	3029.0	s	2835.3	w		
ν_{30t}			3033.9	s				
ν_{33c}	3099.0	s			2844.9	w		
ν_{31t}			3109.5	m				
ν_{34c}, ν_{32t}	3110.0	s	3110.7	m	2882.0	w		
ν_{35c}, ν_{33t}	3118.1	s	3113.1	s	2911.2	w		
ν_{36c}, ν_{34t}	3152.8	s	3152.7	m	2949.7	w		
ν_{37c}, ν_{35t}	3159.6	m	3158.5	m	2981.2	w		
ν_{36t}			3173.7	m				
ν_{38c}	3185.6	m			2990.4	w		

[a] All bands given in cm^{-1} with relative intensities given as w (weak), m (medium), or s (strong). The assigned numbers are listed in order of increasing energy for t (trans) isomer and c (cis).

TABLE 4: Observed and Calculated Low-Energy IR Bands[a]

assigned vib. mode	calculated (cis)		calculated (trans)		IR exptl		IR$_{(cis)}$ Δcalcd−exptl	IR$_{(trans)}$ Δcalcd−exptl
ν_{1t}			347.2	w				
ν_{1c}	353.7	w						
ν_{2c}	380.0	w						
ν_{3c}, ν_{2t}	387.3	w	387.7	w				
ν_{3t}			420.9	w				
ν_{4c}	439.1	m						
*					532.0	w		
ν_{5c}, ν_{4t}	552.9	m	555.8	w	548.7	m	4.2	7.1
ν_{6c}	591.2	w			585.6	w	5.6	

[a] All bands given in cm^{-1} with relative intensities given as w (weak), m (medium), or s (strong). The assigned numbers are listed in order of increasing energy for t (trans) isomer and c (cis). *Not observed.

and the O−N−N−O framework.[17] This remains true for O^2-methyl-1-(*N*,*N*-dimethylamino)diazen-1-ium-1,2-diolate (**3**). Intense infrared-active vibrational modes attributed to deformations of the O−N−N−O framework are calculated (DFT) to be at 1295.3 and 1352.2 cm^{-1} for the cis and trans isomers, respectively. Atomic displacement vector diagrams for these modes are shown in Figure 4. The energies of this band for the two isomers are in a region, 1400 cm^{-1} to 1197 cm^{-1}, which is particularly devoid of bands other than the intense band at 1260.2 cm^{-1} and the medium intensity band at 1222.9 cm^{-1}. As shown in Table 5, there are three calculated bands in this region with substantial intensity: 1295.3 and 1270.2 cm^{-1} for the cis isomer and 1352.2 cm^{-1} for the trans. The predicted energies and intensities more closely correspond to the cis isomer, and the weak peak at 1314.4 cm^{-1} is assigned as the most likely band due to mode 17 of the trans isomer. Although a strong Raman-active framework band at 1352.0 cm^{-1} is expected for the trans isomer, it is most likely to be shifted by 30−40 cm^{-1} as was observed for the cis isomer. As shown in Figure 2, there is indeed a window for this band less than 1350 cm^{-1}, and only the weak band at 1314.4 and the two strong bands of the cis isomer are in this region.

Albeit weak, the appearance of this band in the Raman, along with the above-mentioned bands in the infrared spectra, suggests that the trans isomer might be detected using vibrational spectroscopy. To determine the relative concentrations of the two isomers present in the isolated material, integrated band intensities can be used if their extinction coefficients are similar. Our calculations for the gas phase suggest that these modes do indeed have similar intensities, 87.0 km/mol for the cis (1295 cm^{-1}) and 87.6 km/mol for the trans (1352 cm^{-1}) bands, and so, integration is a good approximation of their relative concentrations. Our previous attempts to estimate the proportion

TABLE 5: Observed and Calculated Fingerprint Region IR Bands[a]

assigned vib. mode	calculated (cis)		calculated (trans)		IR exptl		IR$_{(cis)}$ Δcalcd−exptl	IR$_{(trans)}$ Δcalcd−exptl
*			665.9	m	676.1	m		10.2
ν_{7c}, ν_{5t}	688.3	w	691.2	w				
ν_{6t}			764.1	m				
ν_{8c}	883.4	w			865.6	m	17.8	
ν_{7t}			946.3	m	951.7	s		5.4
ν_{9c}	973.3	s						
*								
ν_{8t}			1001.9	s	1003.8	s		1.9
ν_{10c}	1030.6	m						
ν_{11c}, ν_{9t}	1045.8	s	1040.7	m	1057.4	s	11.6	16.7
ν_{10t}			1064.2	s				
*								
ν_{12c}, ν_{11t}	1097.4	s	1100.7	w				
ν_{13c}	1106.7	w						
ν_{14c}, ν_{12t}	1149.7	m	1150.4	m	1141.0	m	8.7	9.4
ν_{15c}, ν_{13t}	1156.1	w	1158.3	w				
ν_{14t}			1195.8	m	1197.3	w		1.5
*								
ν_{16c}	1213.1	w						
ν_{15t}			1231.6	w				
ν_{17c}, ν_{16t}	1255.9	w	1255.9	w				
ν_{18c}	1270.2	m			1222.9	m	47.3	
ν_{19c}	1295.3	s			1260.2	s	35.1	
*								
ν_{17t}			1352.2	s	1314.4	vw		
*								
ν_{20c}, ν_{18t}	1410.3	w	1413.6	w			10.3	13.6
ν_{21c}, ν_{19t}	1435.9	w	1437.6	w				
ν_{22c}, ν_{20t}	1445.6	w	1447.9	w	1400.0	m		
ν_{23c}, ν_{21t}	1451.9	m	1450.0	w			6.3	8.2
ν_{24c}, ν_{22t}	1456.0	s	1454.2	w	1452.6	m	17.3	19.1
ν_{25c}, ν_{23t}	1470.6	m	1469.4	w	1458.2	m	2.7	3.9
ν_{26c}	1472.9	s			1473.3	m	24.1	
ν_{27c}, ν_{24t}	1474.9	m	1475.3	w	1473.3	m	24.7	24.3
ν_{25t}			1478.6	w	1497.0	s		
ν_{26t}			1488.5	m	1499.6	s		
ν_{28c}	1493.0	m					14.3	
*								
ν_{27t}			1546.0	s	1507.3	s		38.7
ν_{29c}	1573.1	m						

[a] All bands given in cm^{-1} with relative intensities given as w (weak), m (medium), or s (strong). The assigned numbers are listed in order of increasing energy for t (trans) isomer and c (cis). *Not observed.

TABLE 6: Observed and Calculated C−H Stretching Region IR Bands[a]

assigned vib. mode	calculated (cis)		calculated (trans)		IR exptl		IR$_{(cis)}$ Δcalcd−exptl	IR$_{(trans)}$ Δcalcd−exptl
ν_{30c}	2900.1	m						
ν_{31c}, ν_{28t}	3005.9	m	3000.0	s	2724.4	m		
ν_{32c}, ν_{29t}	3026.0	s	3029.0	s	2786.0	m		
ν_{30t}			3033.9	s				
ν_{33c}	3099.0	m			2812.6	m		
ν_{31t}			3109.5	w				
ν_{34c}, ν_{32t}	3110.0	w	3110.7	m	2829.9	m		
ν_{35c}, ν_{33t}	3118.1	m	3113.1	m	2877.3	m		
ν_{36c}, ν_{34t}	3152.8	w	3152.7	w	2906.9	m		
ν_{37c}, ν_{35t}	3159.6	w	3158.5	w	2945.7	m		
ν_{36t}			3173.7	w				
ν_{38c}	3185.6	w			2981.9	m		

[a] All frequencies are in cm^{-1}. Infrared data were obtained on the neat sample using KBr disks and Raman data on glass slides. *Not observed.

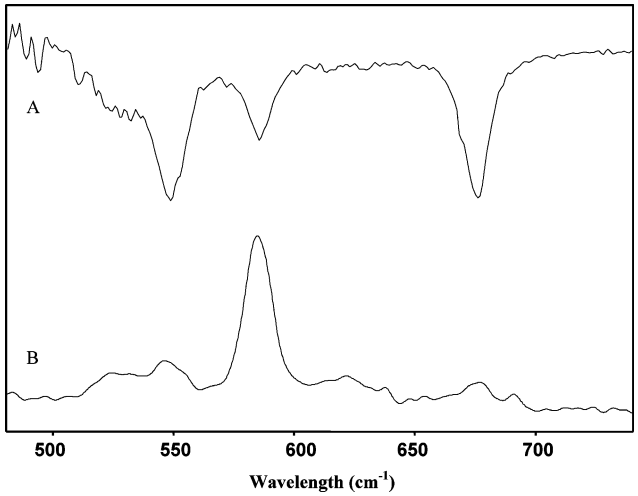

Figure 1. Raman (B) and IR (A) spectra of compound 3 between 425 and 725 cm^{-1}.

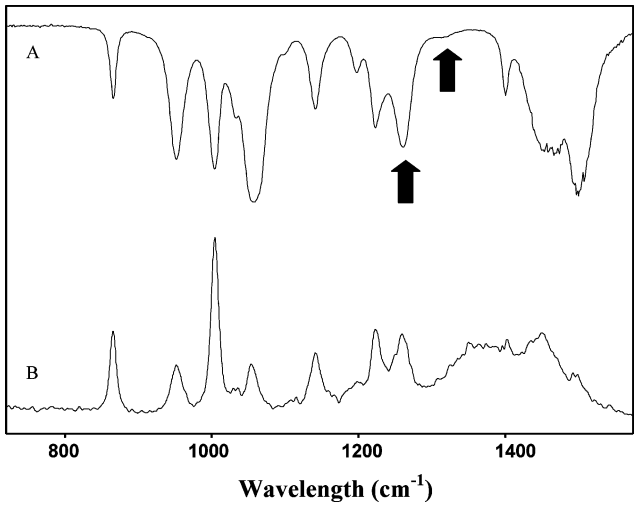

Figure 2. Raman (B) and IR (A) spectra of compound 3 between 775 and 1700 cm^{-1} Arrow in the IR spectrum points to the two integrated bands (see discussion) used to set the limit of *E* to *Z*.

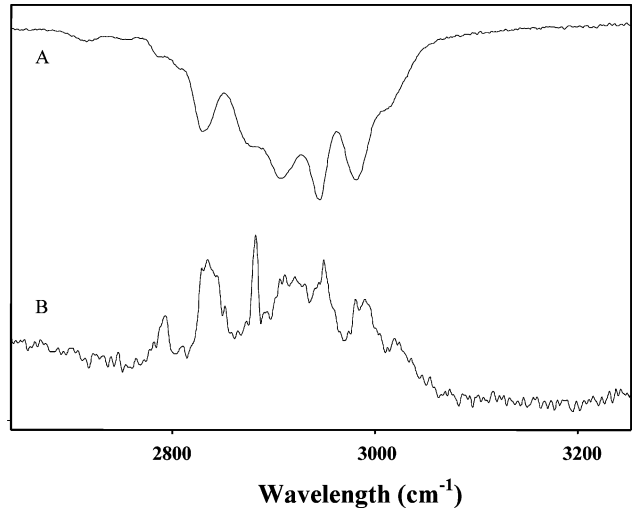

Figure 3. Raman (B) and IR (A) spectra of compound 3 between 2600 and 3240 cm^{-1}.

of *Z* and *E* isomers in a sample of $Me_2NN(O)$═NOMe by ^1H NMR spectroscopy proved to be inconclusive, and it was found that if the *E* isomer is present it must represent <1% of the total.[16] Integration of the 1260 and 1314 cm^{-1} bands in the IR

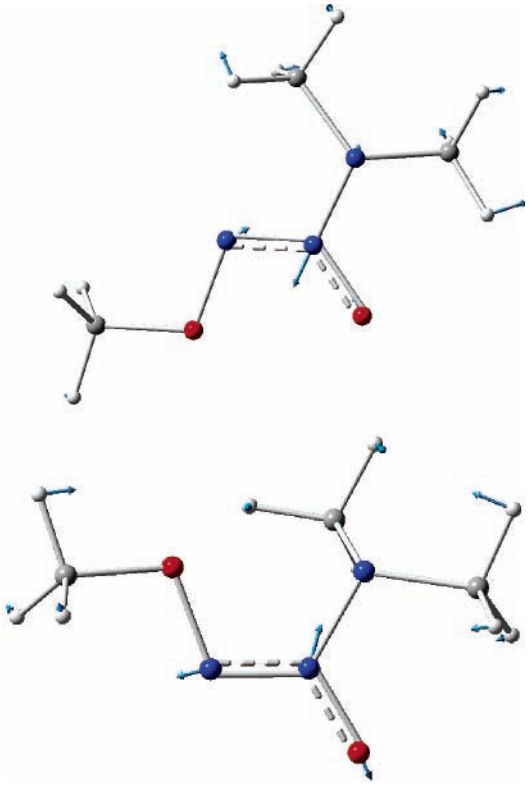

Figure 4. DFT-calculated −O−N═N−O framework modes for *Z* (top) and *E* (bottom) O^2-methyl-1-(*N*,*N*-dimethylamino)diazen-1-ium-1,2-diolate. Displacement vectors for strong IR and Raman bands at 1295.3 and 1352.2 cm^{-1}, respectively, are shown.

suggests that the concentration of trans isomer is $^1/_{200}$ that of the cis diazeniumdiolate. The small quantity of *E* isomer present in the sample poses a challenge for its spectroscopic identification and quantification, and at this time, vibrational spectroscopy appears to give the most sensitive result. Nevertheless, these results are in accord with our prior ^1H NMR results.

C−H Stretching Region. As shown in Figure 3 and summarized in Tables 3 and 6, the theoretically calculated bands for the Raman- and infrared-active C−H stretching modes correlate well to experimental results. This region is attributed to C−H stretching vibrations, and in both the Raman and infrared, the calculated energies are higher than what is observed experimentally. This overestimation of the harmonic vibrational frequencies by ab initio methods is well-known. Radom has suggested that frequencies calculated at the B3LYP/6-31* level be scaled by 0.9614.[25] With this scale factor, there is better agreement between theory and experiment, but we note that the basis sets used here are larger and contain diffuse components as well polarizing components to both the heavy atoms and the hydrogens. Despite this predictable difference in calculated and experimental frequencies, the Raman-active stretching modes parallel the infrared-active bands in position, although they differ in intensity. These bands are all weak in the Raman and medium intensity in the infrared.

Conclusions

Vibrational spectra of the relatively simple diazeniumdiolate $Me_2NN(O)$═NOMe indicate that, if the *E* isomer is present, it corresponds to <0.002% of the total composition. This detection limit is lower than for ^1H NMR, but it is based upon our calculated assignments of band energies and intensities. Although the calculated results match very well those for the known *Z* isomer, reported here, experimental verification of

these assignments for the *E* isomer is limited by the lack of a known preparative route to *E*-$Me_2NN(O)$═NOMe. Clearly, a general synthetic approach to both of these isomers remains an important challenge in this chemistry.

The question of conformational preference and their concentrations in these samples addresses one of the fundamental problems of NO chemistry: How do nucleophiles add to NO, and what is the origin of the observed stereoselectivity? With many secondary amines, the products have remarkably high stereoselectivity for formation of the cis isomer. This reaction is unlikely to be under thermodynamic control, as the calculated (B3LYP/aug-cc-pVDZ)[16] gas-phase energies for *Z* and *E* $Me_2NN(O)$═NOMe differ by only 5.9 kcal mol^{-1}, and with the inclusion of polarized continium model calculations theory for solvation, this value increases to only 6.3 kcal mol^{-1}. For the anion, Houk has calculated an even smaller difference in these energy, $\Delta G = -0.2$ kcal mol^{-1}.[26] The predicted barriers for interconversion for both the anion, $Me_2NN(O)$═NO^-, and $Me_2NN(O)$═NOMe are substantial,[18] with the latter having a value of 37.8 kcal mol^{-1}.[16] Thus, we expect that, if *E*-$Me_2NN(O)$═NOMe is produced, then it should have been observed by the vibrational spectrocopy reported here or by NMR as described before.[16] Clearly, it is not, and thus, the stereoselectivity of the reaction appears to be under kinetic control.

A recent examination of the kinetics of the closely related reaction between triphenylphosphine and nitric oxide[27] determined that the reaction is unimolecular in phosphine and bimolecular in nitric oxide. This rate law is common to many reactions of nitric oxide[28] and can be interpreted as being due to the addition of the substrate to a preformed nitric oxide dimer or to a stepwise reaction where there is a reversible addition of NO to the nucleophile followed by a rate-limiting addition of the intermediate radical, [NuNO·], to the second NO. Ford et al. interpreted their observed solvent dependencies as being due to a stepwise addition of NO,[27] but noted that either mechanism is compatible with the observed kinetics. In the case of the reaction with triphenylphosphine, the products are triphenylphospine and nitrous oxide, and there is no question of stereochemistry. For secondary amines, the stereoselectivity for the *Z* conformation in the product is an important consideration and can be accounted for by the addition of an amine to a preformed NO dimer[29] or by a hypothetical stereoselective radical/radical addition of [NuNO•] to the second NO molecule. A related known example of a stereoselective radical/radical reaction of nitric oxide is its addition to superoxide to produce *Z*-peroxynitrite.[30,31] While amine addition to the cis NO dimer certainly would rationalize the observed stereoselectivity, the binding energy is only 3.1 kcal mol^{-1} at absolute zero,[32] and at higher temperatures, this value is expected to decrease; thus, the amount of dimer at room temperature and moderate pressures, as used in these preparations, is likely to be very low. To understand the reactions of NO in biology, the role of this dimer and its reactivity remain a central problem. In this paper, the surprising degree of stereochemical selectivity in these reactions has been further defined; understanding its origin remains an experimental and theoretical challenge.

Acknowledgment. D.S.B. gratefully acknowledges support from NSERC in the form of a Discovery Grant, and this project has been funded in part by the National Cancer Institute under (contract no. NO1-CO-12400). We thank Dr. Larry Keefer for many enlightening discussions related to this manuscript and its related chemistry.

Supporting Information Available: A complete compilation of calculated energies and intensities for cis and trans isomers of $Me_2NN(O)$═NOMe, at the MP2 and DFT levels of theory, are collected together in one table. This material is available free of charge via the Internet at http://pubs.acs.org.

References and Notes

(1) Hrabie, J. A.; Keefer, L. K. *Chem. Rev.* **2002**, *102*, 1135−1154.

(2) Keefer, L. K. In *Book of Abstracts*, Proceedings of the 215th ACS National Meeting, Dallas, March 29−April 2, 1998; CHED-641.

(3) Bivalacqua, T. J.; Champion, H. C.; De Witt, B. J.; Saavedra, J. E.; Hrabie, J. A.; Keefer, L. K.; Kadowitz, P. J. *J. Cardiovasc. Pharmacol.* **2001**, *38*, 120−129.

(4) Keefer, L. K. *Annu. Rev. Pharmicol. Toxicol.* **2003**, *43*, 585−607, 582 plates.

(5) Hanson, S. R.; Hutsell, T. C.; Keefer, L. K.; Mooradian, D. L.; Smith, D. J. *Adv. Pharmacol.* **1995**, *34*, 383−398.

(6) Saavedra, J. E.; Bohle, D. S.; Smith, K. N.; George, C.; Deschamps, J. R.; Parrish, D.; Ivanic, J.; Wang, Y.-N.; Citro, M. L.; Keefer, L. K. *J. Am. Chem. Soc.* **2004**, *126*, 12880−12887.

(7) Traube, W. *Ber. Dtsch. Chem. Ges.* **1894**, *27*, 1507−1510.

(8) Traube, W. *Ber. Dtsch. Chem. Ges.* **1894**, *27*, 3291.

(9) Arulsamy, N.; Bohle, D. S. *Angew. Chem.* **2002**, *41*, 2089−2091.

(10) Nelsen, S. F.; Teasley, M. F.; Kaftory, M. *J. Org. Chem.* **1988**, *53*, 5930−5933.

(11) Ruzicka, V.; Marhoul, A. *Collect. Czech. Chem. Commun.* **1970**, *35*, 363−366.

(12) Moriya, K.; Iguchi, N.; Makino, K.; Rokushika, S.; Hatano, H. *Can. J. Chem.* **1984**, *62*, 2.

(13) Gotz, M.; Grozinger, K. *Tetrahedron* **1971**, *27*, 4449−4456.

(14) Ogloblin, K. A.; Girbasova, N. V.; Potenkhin, A. A. *J. Org. Chem. USSR (Eng. Trans.)* **1973**, *9*, 2252−2257.

(15) Arulsamy, N.; Bohle, D. S. *Angew. Chem., Int. Ed. Engl.* **2002**, *41*, 2089−2091.

(16) Wang, Y.-N.; Bohle, D. S.; Bonifant, C. L.; Chmurny, G. N.; Collins, J. R.; Davies, K. M.; Deschamps, J. R.; Flippen-Anderson, J. L.; Keefer, L. K.; Klose, J. R.; Saavedra, J. E.; Waterhouse, D. J.; Parrish, D.; Ivanic, J. *J. Am. Chem. Soc.* **2005**, *127*, 5388−5395.

(17) Keefer, L. K.; Flippen-Anderson, J.; George, C.; Shanklin, A. P.; Dunams, T. M.; Christodoulou, D.; Saavedra, J. E.; Sagan, E. S.; Bohle, D. S. *Nitric Oxide* **2001**, *5*, 377−394.

(18) Taylor, D. K.; Bytheway, I.; Barton, D. H. R.; Bayse, C. A.; Hall, M. B. *J. Org. Chem.* **1995**, *60*, 435−444.

(19) Kneipp, K.; Kneipp, H.; Itzkan, I.; Dasari, R. R.; Feld, M. S. *Chem. Rev.* **1999**, *99*, 2957−2976.

(20) Saavedra, J. E.; Srinivasan, A.; Bonifant, C. L.; Chu, J.; Shanklin, A. P.; Flippen-Anderson, J. L.; Rice, W. G.; Turpin, J. A.; Davies, K. M.; Keefer, L. K. *J. Org. Chem.* **2001**, *66*, 3090−3098.

(21) Moller, C. P. M. S. *Phys. Rev.* **1934**, *46*, 618−622.

(22) Pople, J. A.; Binkley, J. S.; Seeger, R. *Int. J. Quantum Chem.* **1976**, *S10*, 1−19.

(23) Becke, A. D. *J. Chem. Phys.* **1993**, *98*, 5648−5652.

(24) Kendall, R. A.; Dunning, J. T. H.; Harrison, R. J. *J. Chem. Phys.* **1992**, *96*, 6796−6806.

(25) Scott, A. P.; Radom, L. *J. Phys. Chem.* **1996**, *100*, 16502−16513.

(26) Dutton, A. S.; Fukuto, J. M.; Houk, K. N. *Inorg. Chem.* **2004**, *43*, 1039−1045.

(27) Lim, M. D.; Lorkovic, I. M.; Ford, P. C. *Inorg. Chem.* **2002**, *41*, 1026−1028.

(28) Gershinowitz, H.; Eyring, H. *J. Am. Chem. Soc.* **1935**, *57*, 985−991.

(29) Zhao, Y.-L.; Bartberger, M. D.; Goto, K.; Shimada, K.; Kawashima, T.; Houk, K. N. *J. Am. Chem. Soc.* **2005**, *127*, 7964−7965.

(30) Woerle, M.; Latal, P.; Kissner, R.; Nesper, R.; Koppenol, W. H. *Chem. Res. Toxicol.* **1999**, *12*, 305−307.

(31) Bohle, D. S.; Hansert, B.; Paulson, S. C.; Smith, B. D. *J. Am. Chem. Soc.* **1994**, *116*, 7423−7424.

(32) Sayos, R.; Valero, R.; Anglada, J. M.; M., G. *J. Chem. Phys.* **2000**, *112*, 6608−6624.